Principles of Design of Magnetic Devices for Attitude Control of Satellites

By M. S. GLASS

Magnetic devices mounted within an orbiting satellite interact with the earth's magnetic field and produce torque to modify the attitude or angular adjustment of the satellite axis of spin. The satellite environment dictates that these devices be designed for minimum weight or minimum power consumption, or a suitable compromise between these two minima. Principles of design of magnetic devices to satisfy these requirements are developed in this paper. The resulting design equations and charts enable the ready optimization of design and selection of preferred materials. While most of this work was directed initially at the Telstar® satellite project, the design charts and formulas are found useful in other areas of magnet design. Methods of magnetic measurement devised for the satellite are discussed.

I. INTRODUCTION

Satellites with directional instrumentation, such as the antenna system of the communications satellites, require attitude control to keep this instrumentation properly on target. For example, a spin imparted to the satellite at time of launch gives it a sort of gyroscopic stability. However, complete attitude control requires some available torque to correct the direction of the spin axis.

In the orbiting satellite the earth's gravitational field is balanced by centrifugal force, leaving the earth's magnetic field as a convenient means for interaction torque. Suitable interaction with the earth's magnetic field can be set up by electromagnets, or by air-core coils of large area, either of which can be turned on or off at will to provide attitude correction as needed. Small permanent magnets can be designed and installed to cancel out residual magnetic moment in the satellite, which if permitted to interact with the earth's field could cause precession of the spin axis. Other miscellaneous torque applica-

tions of magnets in the satellite have been proposed and investigated.

Limitations of payload and of available power in the satellite generally make it necessary to design with quantitative accuracy and to optimize the factors which control weight and power consumption. To this end, the magnet designer may select from various geometries of magnet and coil and from various available materials. This selection and optimization is facilitated by the use of suitable design formulas and charts. In this paper, we review the derivation and illustrative use of such formulas and charts. While the work reported here has been aimed specifically at certain problems of the *Telstar®* satellite, it is evident that the technique of magnet design presented here is applicable to any similar set of problems.

For the convenience of the magnet designer who buys magnets and magnet wire by the pound, measures them in feet, inches, or mils, and measures torque in pound-inches, all of the derived design formulae and graphs are built around the practical units (inches, pounds, oersteds, gauss, etc.). This avoids the necessity of converting units, which is time consuming and can lead to costly errors. There is included for convenience a table of the most frequently used conversion factors (Table I).

II. QUANTITATIVE DESIGN OF AIR-CORE COIL FOR TORQUE

The torque characteristic of the air-core coil is derived from the galvanometer formula which, in some textbooks, is written in MKS units:

$$NIA \text{ (ampere-turn-meter}^2) = \frac{10^7}{4\pi} \frac{T_e}{H_a} \text{ (weber-meters)} \tag{1}$$

TABLE I — CONVERSION FACTORS

1 unit pole (emu)	$= 4\pi$ maxwells
1 oersted	$= \dfrac{10^3}{4\pi}$ ampere turns per meter
	$= 2.02$ ampere turns per inch
1 weber-meter	$= \dfrac{10^{10}}{4\pi}$ emu
	$= \dfrac{8.85 \times 10^3}{4\pi}$ lb-in per oersted
1 newton-meter	$= 10^7$ dyne-cm
	$= 8.85$ lb-in

TABLE II — CHARACTERISTICS OF WINDINGS

	Copper	Aluminum
R(ohms)	$\dfrac{0.75 \times 10^{-6} N^2 P}{A}$	$\dfrac{1.21 \times 10^{-6} N^2 P}{A}$
E(volts)	$\dfrac{0.75 \times 10^{-6} N P (NI)}{A}$	$\dfrac{1.21 \times 10^{-6} N P (NI)}{A}$
W(watts)	$\dfrac{0.75 \times 10^{-6} P (NI)^2}{A}$	$\dfrac{1.21 \times 10^{-6} P (NI)^2}{A}$
Wgt.(lbs.)	$0.321\ AP$	$0.0983\ AP$
(Power × Wgt.)	$0.241 \times 10^{-6} P^2 (NI)^2$	$0.119 \times 10^{-6} P^2 (NI)^2$

NI: Required ampere turns
N: Number of turns used
A: Cross section area of winding (inch²)
   (N times the section area of a single turn)
P: Average length of turn in winding (inch)

and may be written in practical units:

$$NIA(\text{ampere-turn-inch}^2) = 1.667 \times 10^6 \frac{T_o}{H_a} \text{ lb-in/oersted).} \qquad (2)$$

Here T_o is the maximum torque exerted on the coil when its axis is perpendicular to the field H_a, and NIA is the required product of ampere turns and area enclosed by the coil to deliver that amount of torque.

It is convenient to set up a table of formulas from which one may translate the geometry and ampere-turn characteristics of the coil into power and weight requirements. The power and weight will depend upon the winding material used, but practical considerations usually limit this to copper or aluminum. So one may take the weight and resistivity characteristics of copper and aluminum from handbook tables and with the aid of Ohm's Law derive the formulas of Table II. Using (2) and Table II, one may estimate readily the power and weight of an air-core coil to satisfy specified torque requirements. It is evident that copper has the advantage in lower power consumption, but that aluminum offers a greater advantage in weight reduction. If power and weight are of about equal importance, then the power-weight product should be minimized. It is evident that aluminum has a factor-of-two advantage over copper in this characteristic.

III. QUANTITATIVE DESIGN OF MAGNETIZED BARS FOR TORQUE

A magnetized bar, either a permanent magnet or the core of an electromagnet, displays a moment, or normalized torque, proportional to the product of the volume of the bar by the intrinsic induction within the bar. The magnetic moment, M_m, is identified as normalized torque in the familar equation

$$M_m = \frac{T_o}{H_a} \quad \text{(MKS)}, \tag{3}$$

and the relation between magnetic moment, intrinsic induction in the bar, and the geometry of the bar is given by another familiar equation

$$M_m = \frac{B - H}{4\pi} A \cdot S \quad \text{(emu)} \tag{4}$$

in which $B - H$ is the intrinsic induction, A is the cross-section area of the bar at the median plane, and S is the effective distance between poles. For a magnet of length l and diameter d, one may define a shortening factor, $R_S = S/l$, which evaluates the effect of recession of the poles, and rewrite (4) as

$$M_m = \frac{B - H}{4\pi} A l R_S . \tag{5}$$

The shortening factor, R_S, has been evaluated by Okoshi.[1] Okoshi's values are plotted as a function of l/d of the bar in Fig. 1, with a
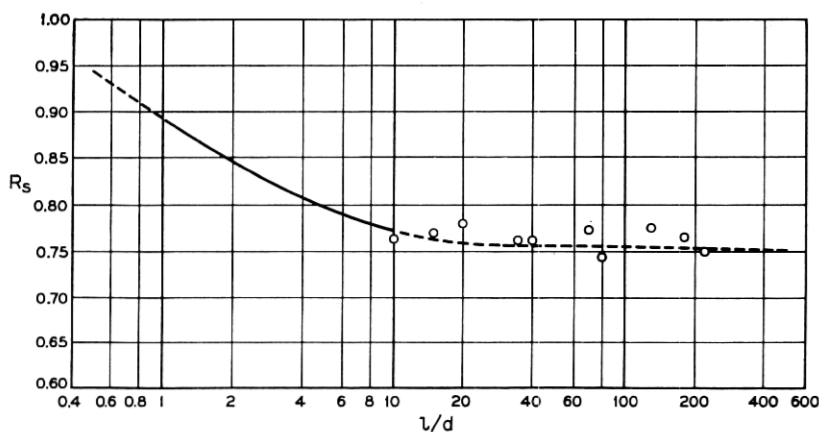

Fig. 1 — Effective shortening of magnets with increasing aspect ratio.

broken line extrapolation guided by experimental data. If one combines (3) and (5) after conversion to practical units, the result is

$$\frac{T_o}{H_a} \text{ (lb-in per oersted)} = 1.55 \times 10^{-6}(B - H)AlR_s \qquad (6)$$

and the required volume of bar to produce a specified magnetic moment is given by rearrangement of (6)

$$\text{Vol (in}^3) = \frac{1}{R_S} \frac{0.866 \times 10^6}{B - H} \frac{T_o}{H_a}. \qquad (7)$$

3.1 Optimum Bar Shape—The Load Factor

When a bar of ferromagnetic material is placed in a field of strength H_o, it assumes a state of magnetization which is commonly described by the equation

$$H = H_o - D_B(B - H)$$

which may also be written

$$D_B = \frac{H_o - H}{B - H}. \qquad (8)$$

Here H_o is the applied magnetizing field, and B and H describe the condition of magnetization within the bar. The demagnetizing factor, D_B, which is partially defined by (8) is used to express the dependence of the intrinsic induction within the bar upon the aspect ratio (l/d) of the bar. It has been tabulated and charted as a function of l/d by Okoshi,[1] Bozorth and Chapin,[2] and others. These sources agree upon the value of D_B for long slender magnets. For shorter magnets, where there is some disagreement, we find the Okoshi data to be in agreement with experiment.

In plotting the characteristics of magnetic materials we normally plot the intrinsic induction $(B - H)$ or the flux density (B) as the dependent variable, and the field strength $(H, \text{ or } H_o)$ as the independent variable. Hence, the ratio

$$\frac{B - H}{H_o - H} = \frac{1}{D_B} = U \qquad (9)$$

becomes the slope of the generalized load line of the magnetized bar. This reciprocal of the demagnetizing factor is found useful in numerous magnetic calculations and possibly deserves a name and symbol of its own. We have elected to call it the loading factor, with the symbol U,

and have plotted it as a function of l/d in Fig. 2. In the electromagnet core operating below saturation, H is generally negligibly small compared with either B or H_o, and the expression for the loading factor reduces to $U = B/H_o$. In the permanent magnet, H_o disappears and the expression for loading factor becomes $U = (B - H)/(-H)$. For long magnets, $(l/d > 5)$ H is negligibly small compared with B, and the loading factor is further simplified to $U = B/(-H)$. In this restricted form the loading factor is identified with the "permeance coefficient" and similar terms used in the literature of permanent magnets.

In Fig. 3 we illustrate the application of the loading factor to the analysis of permanent magnets and electromagnets. For this illustration each is assumed to have $l/d \cong 33$ so that the loading factor, $U \cong 400$. In the permanent magnet (Remendur) the magnetomotive force
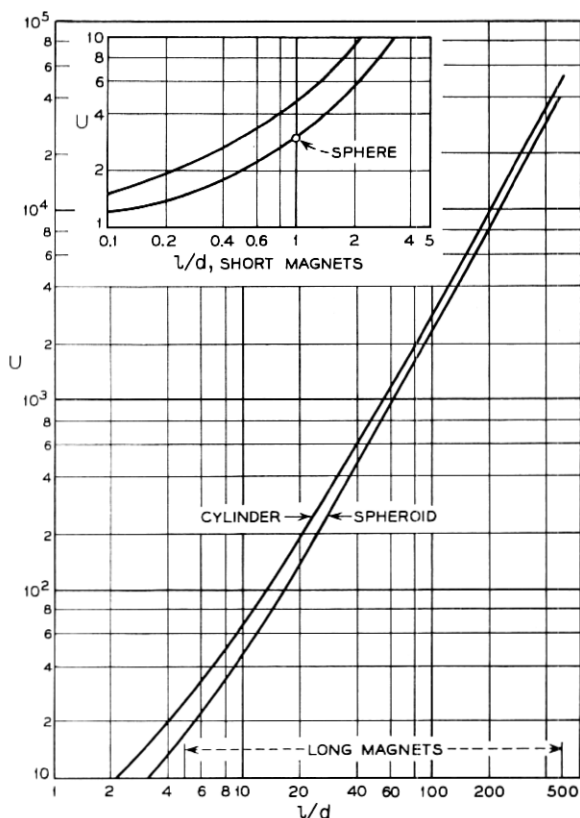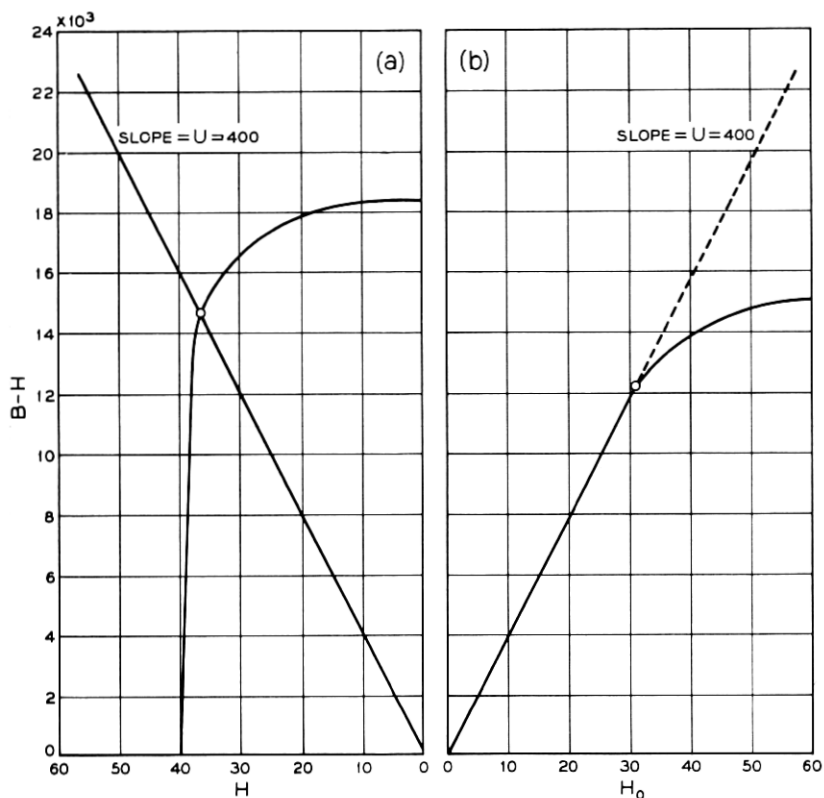

Fig. 2 — Variation of load factor with aspect ratio.

Fig. 3 — Application of load factor to magnet design: (a) permanent magnet (Remendur 38), (b) electromagnet (Permalloy 45 core).

is generated within the magnet and varies with the loading of the magnet as indicated by the B, H curve. (Here H is sufficiently small so that B is indistinguishable from $B - H$). The operating point is determined by the intersection of the B, H curve with the load line of slope U. This is a fixed point for a particular magnet with a particular condition of magnetization. The conditions of Fig. 3 were chosen to match the characteristics of Remendur. In the electromagnet when operated below saturation, H is negligibly small so the load line represents the relation between flux B in the bar, and applied field, H_o, up to the region (around $B = 10,000$ for Permalloy 45) where the core material starts saturation, and the characteristic starts deviating from the straight load line.

3.2 Design of Permanent Magnets for High Torque-Weight Ratio

The weight of the magnet in pounds is

$$W_m = Al\rho, \tag{10}$$

in which ρ is density of magnet material in lbs/in^3. One may combine (10) with (6) to obtain

$$\frac{T_o}{W_m H_a} = \frac{1.155 \times 10^{-6}}{\rho} (B - H)R_S . \tag{11}$$

Here the left-hand side of (11) is the normalized torque-weight ratio. The design objective is to maximize this ratio.

The dependence of the operating point of the permanent magnet upon the load factor, U, has been illustrated in Fig. 3. On similar charts one may plot intrinsic induction $(B - H)$ as a function of field (H) for various magnet materials as in Fig. 4. Values of B and H for these plots may be derived readily from the regular demagnetization curves supplied by magnet manufacturers. Then, for a particular value of
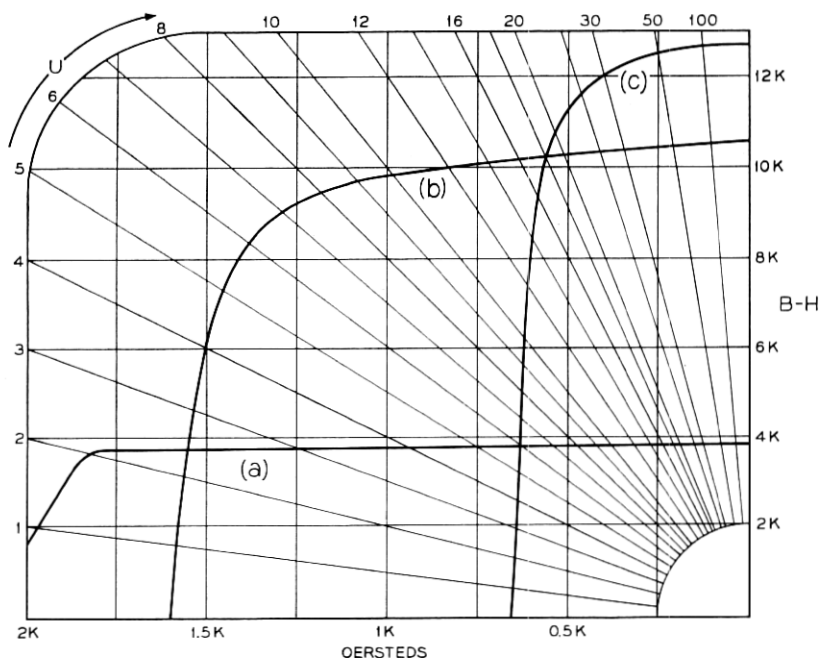

Fig. 4 — Intrinsic induction of permanent magnets; (a) directional grain ceramic, (b) Alnico 9, (c) Alnico 5.
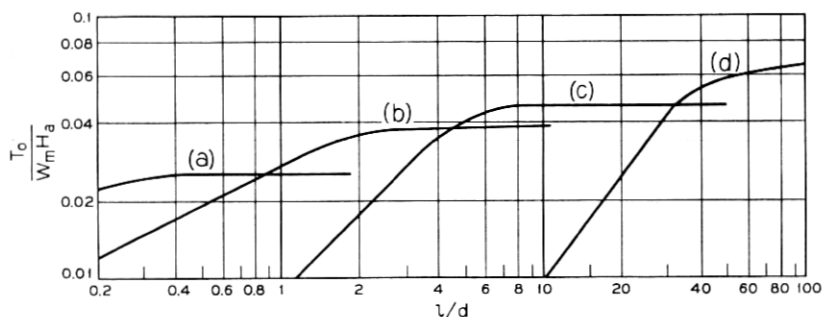
Fig. 5 — Variation of torque-weight ratio with aspect ratio; (a) directional grain ceramic, (b) Alnico 9, (c) Alnico 5, (d) Remendur 38.

l/d one may pick off the corresponding value of U from Fig. 2, and using this as the slope of the load line may find the value of $(B - H)$ for a particular magnet material at the point of intersection. This value of $(B - H)$ and the value of ρ appropriate to the material may be inserted in (11) to give the normalized torque-weight ratio. For example, at $l/d = 4$, $U \cong 17.5$. The load line of that slope intersects the intrinsic induction curve for Alnico 5 at $(B - H) \cong 10,000$. Inserting this value and the value of R_S in (11) and using $\rho = 0.26$ for Alnico, one obtains

$$\frac{T_o}{W_m H_a} = 3.6 \times 10^{-2}. \tag{12}$$

Repeating this procedure for various values of l/d and for various materials, one can assemble the necessary data to plot the curves of Fig. 5.

It is evident that for each magnet material there is a value of l/d above which the torque-weight ratio is essentially constant, and below which the torque-weight ratio falls off rapidly with decreasing l/d. This follows the shape of the demagnetization curves of Fig. 4. This value of l/d is large for magnets having low coercivity, and small for magnets having high coercivity. One would normally design the magnet to operate on the flat part of the characteristic to obtain high torque-weight ratio.

3.3 Design of Electromagnets for Torque

The electromagnet is assumed to consist of a cylindrical core of ferromagnetic material with a solenoid wound around it. The design formula for the core is the same as that for the permanent magnet and

is given in (7). This gives the required volume to produce a specified moment, operating the core at a specified value of flux density. The ampere-turn requirements are derived as follows.

In terms of equivalent ampere turns, the applied field is given by

$$H_o = \frac{NI}{2.02l}. \tag{13}$$

If, as is usually the case in the electromagnet, H is negligibly small compared with H_o, then one may combine (8) and (13) to obtain

$$NI = 2.02lD_B(B - H). \tag{14}$$

If one multiplies each side of (14) by $(Al)^{\frac{1}{3}}$ and collects terms, one obtains

$$NI = 2.02 \frac{l}{(Al)^{\frac{1}{3}}} D_B(B - H)(Al)^{\frac{1}{3}}. \tag{15}$$

But,

$$\frac{l}{(Al)^{\frac{1}{3}}} = (l/d)^{\frac{2}{3}}(\pi/4)^{-\frac{1}{3}}. \tag{16}$$

Combining (15), (16), and (6)

$$NI = 1.9 \times 10^6 (Al)^{-\frac{2}{3}} \frac{T_o}{H_a} \frac{1}{R_S} D_B(l/d)^{\frac{2}{3}}. \tag{17}$$

Since D_B and R_S are functions of aspect ratio (l/d) one may define an aspect ratio factor,

$$F_a = D_B(R_S)^{-1}(l/d)^{\frac{2}{3}} \tag{18}$$

and chart it as a function of (l/d) as in Fig. 6. Then combining (17) and (18), gives

$$NI = 1.9 \times 10^6 \frac{F_a}{(Al)^{\frac{2}{3}}} \frac{T_o}{H_a}. \tag{19}$$

For any proposed geometry of an electromagnet with specified value of magnetic moment (T_o/H_a) the ampere-turn requirement may be determined from (19) and then translated into power and weight requirements by reference to Table II.

3.4 The Semi-Permanent Magnet

A permanent magnet material with low coercivity and high remanence, as exhibited by Remendur in Fig. 3, offers the inviting possi-
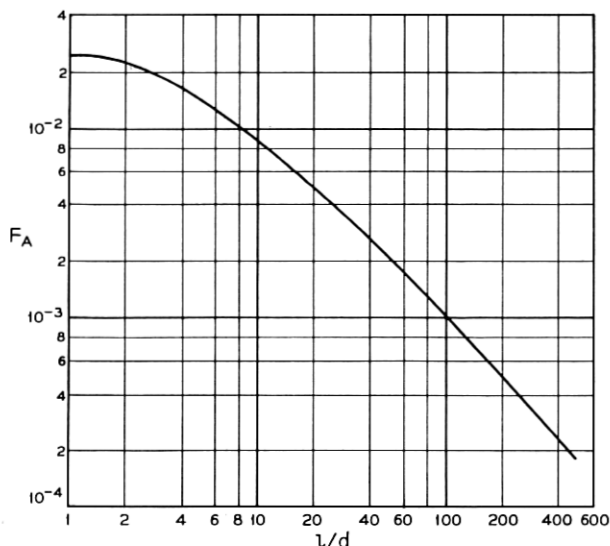
Fig. 6 — The aspect ratio function (F_a).

bility of easy magnetization and reversal of field by means of short pulses of current through a winding. Between pulses it acts as a permanent magnet, with polarity determined by the direction of the preceding pulse. Thus, it provides a switchable field with very low expenditure of power. It requires, however, for complete demagnetization, or "knock-down," much more sophisticated circuitry. Also, the certainty of complete demagnetization from an applied pulse or series of pulses, depends to a considerable extent upon the preceding history of the magnet. For this reason, it is not likely to replace readily the simple air-core coil or electromagnet unless the available power is so severely limited as to justify the added circuit development effort.

IV. INTERCOMPARISON—AIR-CORE COILS AND ELECTROMAGNETS

In the preceding sections we have developed design formulas and design graphs which enable us to estimate with fair quantitative accuracy the size and weight of various magnetic structures to satisfy torque requirements as specified. Intercomparison of the air-core coil and electromagnet offers an interesting illustration of the use of these techniques. We consider a typical example which assumes a spherical satellite of 45 inches effective diameter in which there is required an available magnetic moment of 0.2 lb-in per oersted which can be

turned on or off at will. It is further assumed that an upper limit of nine pounds weight and twelve watts power consumption is to be imposed upon the magnetic circuitry.

First, we assume that an air-core coil is laid out around the equator of the satellite to enclose maximum area, and that this area is

$$A = \frac{\pi}{4} (45)^2 = 1590 \text{ in}^2.$$

Substituting this value of A in (2) gives the required ampere turns,

$$NI = \frac{1.667 \times 10^6}{1.590 \times 10^3} 0.2 = 210.$$

The average length per turn of winding is $45\pi = 141$ inches. Using the formula for aluminum from Table II we can show that the power × weight product is

$$\text{power} \times \text{weight} = 0.119 \times 10^{-6}(141)^2(210)^2 = 105.$$

If we use the total weight allowance of nine pounds for the winding then the required power is

$$\text{power} = \frac{105}{9} = 11.7 \text{ watts.}$$

This is within the permitted 12 watts, so we have shown that it is feasible to use an equatorial coil.

Turning now to the design of the electromagnet, one inserts $T_o/H_a = 0.2$ and $(B - H) = 10,000$ in (7) to show that the required volume of core material is

$$\text{vol} = \frac{0.866 \times 10^6}{10^4} 0.2 = 17.32 \text{ in}^3.$$

Assuming density of 0.26 lbs/in³, the core will weigh 4.5 pounds.

The characteristics of the winding, however, are closely dependent upon the aspect ratio of the core. To illustrate this point we consider two shapes, one to be 10 inches long, the other to be 45 inches long to just fit in along the spin axis of the satellite. For the 10-inch core,

$$\frac{\pi}{4} (10)d^2 = 17.32; \quad d = 1.485''; \quad l/d = 6.73; \quad F_a = 0.1.$$

Substituting these values in (19) gives the required ampere turns,

$$NI = \frac{1.9 \times 10^6}{(17.32)^{\frac{1}{3}}} (0.2)(0.1) = 5640.$$

If we assume the average diameter of the winding is 1.6 inches then the average length of turn, $P = 5.05$ inches. We insert these numbers into the power × weight formula for aluminum in Table II and obtain

$$\text{power} \times \text{weight} = 0.119 \times 10^{-6}(5.05)^2(5.64)^2 \times 10^6 = 97.$$

If we let the winding weigh 4.5 pounds to use up the residue of the weight allotment, then the power requirement is 21.5 watts. Since the maximum allowable power dissipation is 12 watts, it is evident that the 10-inch electromagnet, as described, cannot satisfy the requirements.

For the 45-inch core:

$$\frac{\pi}{4}(45)d^2 = 17.32; \qquad d = 0.7''; \qquad l/d = 64; \qquad F_a = 0.012$$

and substituting these numbers in (19) gives the required ampere turns,

$$\text{NI} = \frac{1.9 \times 10^6}{(17.32)^{\frac{2}{3}}}(0.2)(0.012) = 680.$$

If we assume that the average diameter of the winding is 0.85 inch, then the average length of turn, $P = 2.67$ inches, and

$$\text{power} \times \text{weight} = 0.119 \times 10^{-6}(2.67)^2(680)^2 = 0.39.$$

So we may use 0.5 pound of winding to bring the total weight only to five pounds, and the required power will be only 0.78 watt. This illustrates the advantage of the long slender electromagnet over the short one for purposes of producing torque.

It is evident that the specified conditions of the example can be satisfied by the equatorial coil or by the long slender electromagnet. On the basis of the calculated results one might well prefer the electromagnet, which satisfies the requirements with a substantial saving of power and weight. However, other factors must be considered. It is not likely to be convenient to mount the magnet full length along the spin axis because of interference with other equipment. In a core of this length, a very small amount of residual magnetization after removal of current will result in a considerable magnetic moment, rather than the desired zero magnetic moment which is characteristic of the de-energized air-core coil. The weight distribution of the electromagnet along the spin axis decreases the spin stability, while the weight distribution of the equatorial coil enhances the spin

stability of the satellite. For these and other reasons the equatorial coil remains a favored method of attitude control in the communications satellite.

V. OPTIMUM DESIGN OF PERMANENT MAGNETS FOR FRICTION DAMPING

There have been various proposals to provide friction damping of roll or precession of the spin axis by mounting a small magnet within a hollow spherical enclosure attached to the satellite. The magnet would tend to maintain its alignment in the earth's field and to provide damping through friction contact with the interior of the sphere. For this application, if it exists, or for any similar application, one would wish to design for maximum normalized torque and minimum normalized period of oscillation in the field and within the confines of the sphere.

5.1 Design for Maximum Moment within Limiting Spheres

Referring to (6) and dividing through by D^3 where D is diameter of sphere in inches, and $D^3 = (d^2+l^2)^{3/2}$,

$$\frac{T_o}{H_a D^3} = 0.91 \times 10^{-6} l/d[1 + (l/d)^2]^{-\frac{3}{2}}[B - H]R_S . \tag{20}$$

The relation expressed by (20) is displayed in Fig. 7 for the same magnet materials for which the torque-weight relation was shown in Fig. 5.

5.2 Design for Minimum Period of Oscillation within Circumscribed Sphere

A magnet used to damp out roll or precession should have a natural period of oscillation in the earth's field much shorter than the period of the motion it is to damp out. This would suggest a magnet designed to have minimum period of oscillation with a spherical enclosure.

The moment of inertia of the cylindrical magnet around a diameter through its equator is given by

$$M_i = \frac{\pi}{4} \frac{\rho}{g^*} ld^2 \left[\frac{d^2}{16} + \frac{l^2}{12}\right] \tag{21}$$

and dividing through by D^5,

$$\frac{M_i}{D^5} = 42.6 \times 10^{-6} \rho(l/d) \frac{[3 + 4(l/d)^2}{[1 + (l/d)^2]^{5/2}} . \tag{22}$$
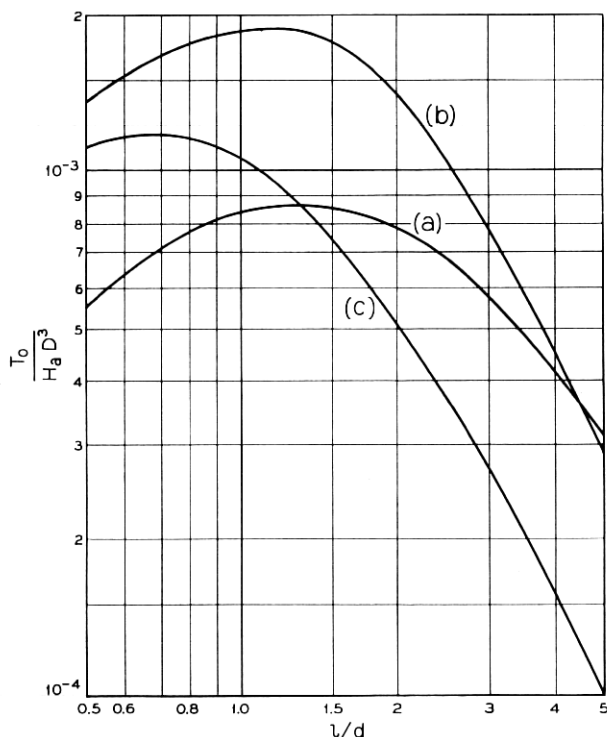
* $g = 384$ in/sec/sec.

Fig. 7 — Normalized moment within limiting sphere; (a) ceramic, (b) Alnico 9, (c) Alnico 5.

Combining (20) and (22) and collecting terms, one obtains,

$$\frac{M_i}{T_o} \frac{H_a}{D^2} = \frac{46.8\rho[3 + 4(l/d)^2]}{R_s[B - H][1 + (l/d)^2]}. \tag{23}$$

The period of oscillation is given by

$$\tau = 2\pi\sqrt{\frac{M_i}{T_o}} \text{ sec}. \tag{24}$$

Combining (23) and (24) yields,

$$\frac{\tau\sqrt{H_a}}{D} = 42.8\sqrt{\frac{\rho[3 + 4(l/d)^2]}{R_s[B - H][1 + (l/d)^2]}}. \tag{25}$$

This normalized period of oscillation is displayed graphically as a function of l/d in Fig. 8. In designing a magnet for friction damping
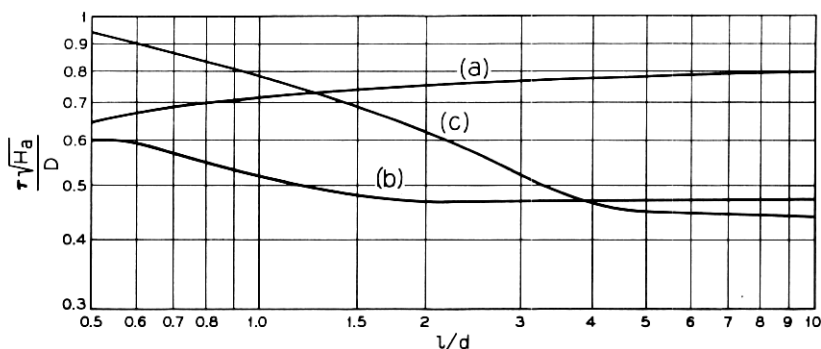
Fig. 8 — Period of oscillation within limiting sphere; (a) ceramic, (b) Alnico 9, (c) Alnico 5.

one would probably select the best compromise between maximum torque displayed in Fig. 7 and minimum period of oscillation as shown in Fig. 8. This would suggest the use of Alnico 9 and design for $l/d \cong 1.5$.

VI. CHARACTERISTICS OF SPHERICAL AND SPHEROIDAL MAGNETS

The spheroids are a family of solids the surfaces of which are generated by ellipses revolving around an axis. Revolution around a major axis generates a prolate spheroid for which $l/d > 1$. Revolution around a minor axis generates an oblate spheroid for which $l/d < 1$. Revolution of a circle around a diameter generates a sphere for which $l/d = 1$.

Values of load factor, U, for spheroids are plotted in Fig. 1. The volume of the spheroid is only two thirds that of a cylinder having the same l and d, so (11) becomes, for spheroids,

$$\frac{T_o}{W_m H_a} = \frac{1.733 \times 10^{-6}(B - H)R_S}{\rho}. \qquad (26)$$

From solutions of (26) one may plot curves for normalized torque-weight ratio. In Fig. 9 we show a curve for spheroids of Alnico together with a curve for cylinders of Alnico borrowed from Fig. 5. While the spheroids show a somewhat better torque-weight ratio than the cylinders, it is doubtful whether the advantage is sufficient to offset the added cost of shaping and mounting.

The sphere might have unique advantages mounted in a spherical enclosure for friction damping. For the sphere of diameter D, one may rewrite (6)

$$\frac{T_o}{H_a} = 1.155 \times 10^{-6}(B - H)\frac{\pi}{4}D^3 R_S . \tag{27}$$

Dividing through by D^3 and inserting value of R_S, gives

$$\frac{T_o}{H_a D^3} = 0.81 \times 10^{-6}(B - H). \tag{28}$$

This is an expression for the total normalized torque that can be packed into a specified spherical enclosure. Solutions of (28) for various magnet materials are collected in Table III. The moment of inertia of the sphere is

$$M_i = 0.1MD^2 = 0.1\frac{\pi}{6}D^5\frac{\rho}{g}. \tag{29}$$

Combining (27) and (29)

$$\frac{M_i H_a}{T_o} = \frac{0.1(\pi/6)D^5\rho}{1.155 \times 10^{-6}(\pi/4)(B - H)D^3 g R_S} = \frac{150\rho D^2}{(B - H)R_S}. \tag{30}$$

Combining (24) and (30)

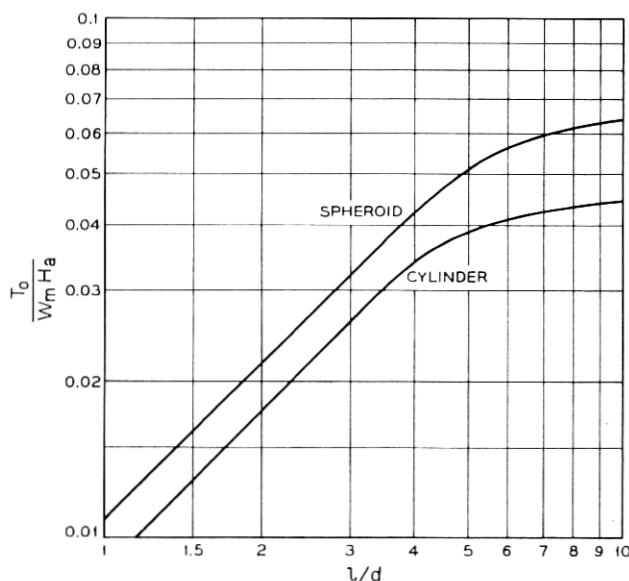$$\frac{\tau\sqrt{H_a}}{D} = 24.5\pi\sqrt{\frac{\rho}{(B - H)R_S}}. \tag{31}$$

Fig. 9 — Comparison, spheroidal and cylindrical magnets of Alnico 5.

TABLE III — MAGNETIC CHARACTERISTICS OF SPHERES

Material	ρ	$(B - H)$	$\dfrac{T_o}{W_m H_a}$	$\dfrac{T_o}{H_a D^3}$	$\dfrac{r\sqrt{H_a}}{D}$
Ceramic	0.15	3700	3.81×10^{-2}	3.0×10^{-3}	0.514
Alnico 9	0.26	4600	2.73×10^{-2}	3.74×10^{-3}	0.613
Alnico 5	0.26	1900	1.13×10^{-2}	1.54×10^{-3}	0.955

Equations (26), (28), and (31) define for the sphere the same normalized quantities which are plotted for the cylinder in Figs. 5, 7, and 8. Solutions of these equations for various magnet materials are listed in Table III. The combination of the table and the three figures gives all the information required to select the preferred material and geometry for a specified application and to arrive at a quantitative design of the magnet.

VII. SATELLITE MAGNETIC MEASUREMENTS

Satellites with spin stabilization introduce two magnetic measuring problems—measurement of "drag" and measurement of residual moment. The "drag" results from eddy currents induced in the rotating metal shell of the satellite by the earth's magnetic field. The energy dissipated in these eddy currents must be derived from the rotational energy of the satellite, and there results a decay of the spin rate. One wishes to evaluate the rate of this decay to forecast when the spin rate will fall below the minimum required for stability. The moment measurement is to detect any residual magnetic moment perpendicular to the axis of spin which will interact with the earth's magnetic field to induce precession of the spin axis. After an accurate measurement this moment is canceled out by mounting in the satellite a small permanent magnet of equal moment and opposite polarity. Both measurements—drag and moment—can be made conveniently with a specially designed coil array.

7.1 *The Telstar® Coil Array*

The drag test requires a reasonably uniform field over the volume of the satellite. A paper analysis reveals that this can be provided by an array of coils of reasonable size with a particular distribution of ampere turns. Two coils, each of radius r, and of N turns are spaced $\pm r/4$ from an assumed zero point on a common axis. Two other coils, each of radius r, and $7N/3$ turns, are spaced $\pm r$ from the assumed

zero along the common axis. The coils are connected in series to run at the same current so that the outer coils have effectively 7N/3 times as many ampere turns as the inner pair. The arrangement of coils and the resulting distribution of field along the axis are shown in Fig. 10.

It was established by measurements that the region of uniform field extended out radially from the axis to include a spherical volume, the radius of which is roughly two thirds the radius of the coils. Hence, an array of coils five feet in diameter easily provided uniform field over the volume of the satellite. (If a conventional Helmholtz array were used the coils would have to be about 10 feet in diameter to achieve reasonably uniform field over the same volume.) This array was mounted on a turntable and rotated around the satellite which was supported by a calibrated torque suspension. From the result of this drag measurement it was possible to calculate the rate of decay of satellite spin in the earth's magnetic field.

7.2 Measurements of Magnetic Moment

The magnetic moment perpendicular to the spin axis of the satellite was measured by rotating it within a coil array similar to the one used for drag tests except that the windings were connected to an integrating fluxmeter. One reasons intuitively that if a magnetic object is aligned parallel to the axis of the coils and rotated 180°, it will give a deflection of the integrating fluxmeter proportional to the moment, and that the proportionality constant will be unaffected by the position
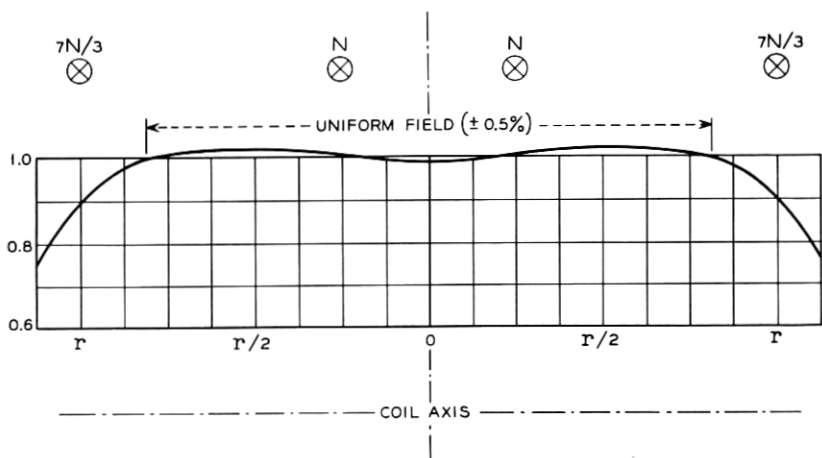

Fig. 10 — Field distribution along axis of *Telstar*® array.

of the magnet in the array as long as it is within the volume in which the array produces uniform field. This intuitive reasoning has been confirmed by various measurements. The proportionality constant for the array is established by calibration with a small air-coil, of known NIA for which the moment can be calculated from (2). A two-to-one scale down of the array has proved to be convenient for bench measurements of magnetic moment of small magnetic objects.

VIII. ACKNOWLEDGMENT

The author is indebted to Mr. L. Rongved for stimulating discussions of the dynamics of the orbiting satellite.

APPENDIX

Definition of Symbols

The following letter symbols have been adopted for use in this paper.

A = section area of magnet or winding.
B = flux density.
$(B - H)$ = intrinsic induction,
d = diameter of magnet.
D = diameter of enclosing sphere.
D_B = demagnetizing factor.
F_a = aspect ratio factor, as defined in text.
g = gravity (384 in/sec/sec).
H = field strength in magnet.
H_a = ambient field, or field of interaction.
H_o = applied magnetizing field.
l = length of magnet.
M = mass.
M_i = moment of inertia.
M_m = magnetic moment.
NI = ampere turns.
R_S = shortening ratio, from recession of poles.
T_o = torque between magnet and perpendicular field.
τ = period of mechanical oscillation.
U = load factor, reciprocal of demagnetizing factor.

REFERENCES

1. Okoshi, Takanori, Demagnetizing Factors of Rods and Tubes Computed from Analog Measurements, J.A.P., *36*, August, 1965, pp. 2382–2387.
2. Bozorth, R. M., and Chapin, D. M., Demagnetizing Factors of Rods, J.A.P., *13*, May, 1942, pp. 320–326.